Relationship between Cognitive Impairment and Retinal Morphological and Visual Functional Abnormalities in Alzheimer Disease

Pervin K. Iseri, MD, Özgül Altinaş, MD, Tomris Tokay, MD, and Nurşen Yüksel, MD

Background: There is conflicting evidence as to whether Alzheimer disease (AD) is accompanied by loss of retinal ganglion cells. To evaluate this issue, we have used optical coherence tomography (OCT) to assess the thickness and volume of the retina. We have also sought to correlate our findings with visual function and cognitive impairment.
Methods: We evaluated 28 eyes of 14 patients with AD and 30 eyes of 15 age-matched control subjects. In these two groups, we measured retinal nerve fiber layer (RNFL) thickness, macular thickness, and macular volume with OCT, visual function through latency of the pattern visual evoked potential (VEP) signal, and cognitive impairment through the Mini-Mental State Examination (MMSE).
Results: The parapapillary and macular RNFL thickness in all quadrants and positions of AD patients were thinner than in control subjects. The mean total macular volume of AD patients was significantly reduced as compared with control subjects ($P < 0.05$). Total macular volume and MMSE scores were significantly correlated. No significant difference was found in the latency of the VEP P100 of AD patients and control subjects.
Conclusions: Our study confirms some other studies in showing that in AD patients there is a reduction of parapapillary and macular RNFL thickness and macular volume as measured by OCT. The reduction in macular volume was related to the severity of cognitive impairment.

(*J Neuro-Ophthalmol* 2006;26: 18–24)

Alzheimer disease (AD) is the most common degenerative dementia and causes a progressive decline in cognitive function. In most cases, an episodic memory deficit is the predominant initial complaint. As time passes, changes in daily living activities, cognitive functions, and visual disturbances supervene.

Visual disturbances consist of impairment in spatial contrast sensitivity (1), motion perception (2,3), color discrimination (4), and blurred vision (5). Several recent articles have attributed the visual dysfunction in AD to damage in primary visual cortex and to degeneration of higher cortical areas (6–8). Other studies have shown evidence of pre-cortical involvement on the basis of reduction in the number of retinal ganglion cells and axons of the optic nerve (9,10). In contrast to these reports, some histopathologic studies have shown no retinal nerve damage in AD (11,12). Although recent studies have used sophisticated imaging techniques, such as optical coherence tomography (OCT), scanning laser polarimetry, and pattern electroretinography (PERG), to assess the morphologic and functional changes of the retina in AD, disagreement about retinal involvement persists (13–15).

The macula is defined anatomically as that region of the retina where the ganglion cell layer has a thickness of more than one cell. The ganglion cells and retinal nerve fiber layer (RNFL) contribute 30% to 35% of retinal thickness in the macula, where the ganglion cells are known to be most concentrated (16). Blanks et al (17) histologically observed a total decrease of 25% of neurons in the ganglion cell layer at the level of the fovea/parafoveal retina in AD. The greatest decrease was in the foveal region. To our knowledge, no previous studies have investigated macular thickness and volume in living AD patients.

OCT is a relatively new non-invasive, non-contact, transpupillary imaging technology that provides high-resolution cross-sectional images of the retina. OCT has been reported to be useful in assessing glaucoma, diabetic neuropathy, and macular edema (18–22).

The aim of this study was to investigate whether a correlation exists between structural (RNFL thickness, macular thickness and volume) and functional (visual evoked potential [VEP]) measures and cognitive impairment in AD.

Departments of Neurology (PKI, TT) and Opthalmology (ÖA, NY), Kocaeli University Medical School, Kocaeli, Turkey.

Address correspondence to Pervin K. Iseri, MD, Kocaeli University, Department of Neurology, Derince Kocaeli 41100 Turkey; E-mail: pervin.iseri@gmail.com

METHODS

Patient Accrual

We compared 28 eyes of 14 patients with AD to 30 eyes from 15 age-matched control subjects. The AD patients were obtained from the Kocaeli University Neurology Department Dementia Clinic; the control subjects were obtained from the Kocaeli University Eye Diseases Department General Clinic, Kocaeli, Turkey. The patients met criteria for probable AD set by the National Institute of Neurological and Communicative Disorders and Stroke-Alzheimer's Disease and Related Disorders Association (NINCDS-ADRDA) (23) and DSM-IV. AD patients had mild and moderate cognitive impairment according to the Clinical Dementia Rating (CDR) scale (24). All participants were free of ocular disease and systemic disorders affecting vision. Informed consent of AD patients was obtained from their first-degree relatives. The research followed the tenets of the Declaration of Helsinki, and the protocol was approved by the local ethics committee.

Neurological Assessments

Each AD patient underwent a detailed neurological examination including laboratory, neuro-imaging evaluations, and psychometric testing. The control subjects also underwent a detailed neurological examination to rule out the presence of cognitive impairment. We excluded patients with dysmetabolic diseases, a history of alcohol abuse, psychiatric disorders, or other neurological diseases. Mini-Mental State Examination (MMSE) (25), Blessed short orientation, and Clock drawing tests for clinical evaluation were used to assess cognition in AD and control subjects.

Ophthalmological Assessments

All AD patients and control subjects underwent a complete ophthalmologic examination, including assessment of visual acuity, refraction, ocular motility, pupillary reflexes, anterior and posterior segment biomicroscopy, applanation tonometry, dilated fundus examination, and Octopus 101 perimeter program G2 visual field testing. The visual field results were uniformly normal in AD and control subjects. All participants had a corrected visual acuity of 5/10 or better with a refractive error between $\pm$ 3 spheric diopters and intraocular pressures less than 22 mmHg. Eyes with posterior pole pathology such as macular degeneration, glaucoma suspect, or glaucoma, or patients with media opacification such as cataract that prevented ocular and OCT examination were excluded.

Visual Evoked Potential Examination

All AD patients and control subjects underwent VEP examination. The VEP was generated using a black-and-white checkerboard pattern on a television monitor with a dimension of 5 $\times$ 5 cm for every check under the following conditions: contrast 95%, check size subtense 50', reversal rate 2 sec^{-1}, mean luminance 12 $Cd.m^{-2}$ field size 17° $\times$ 14°. One hundred stimulus epochs of 200 msn were obtained in each average and the amplifier bandwidth was 1–100 Hz.

Patients sat one meter away from the monitor. Ag/AgCl cup-shaped electrodes fixed with collodion were placed over the left and right occiputs at O1 and O2 with a common reference at Fpz and a ground on the left arm. The patients' gaze was fixed on a point at the center of the television monitor monocularly. The bioelectric signal was filtered (bandpass 0.5–200 Hz). Two hundred responses were averaged for every trial (Neuropack Nihon Kohden, MEB-5504 K, Tokyo, Japan). The analysis time was 250 milliseconds. Sweep length was 300 milliseconds (30 msec/div) and stimulus rate was 1 Hz. The normal range of P100 peak latency is 100.26 $\pm$ 7.04 milliseconds based on testing of normal controls in our laboratory. Peak latencies of the P100 component were measured.

Optical Coherence Tomography Examination

All AD patients and control subjects underwent OCT examination. The RNFL thickness, and macular thickness and volume were measured by OCT Model 3000 unit (Model 3000, software version A1.1, Carl Zeiss Meditec, Inc., Dublin, California, USA) after pupillary dilatation. Tomography images were constructed from a series of axial reflectance profiles (A-scans) over 2 mm of depth in less than 1 second. Retinal thickness and RNFL thickness were calculated by processing the cross-sectional images using computer algorithms to detect boundaries by searching each A-scan for the highest rates of changes in reflectivity. The software allows the mapping of the thickness data according to quadrant-by-quadrant and clock-hour analyses. Retinal thickness was determined by computer as the distance between the first reflection at the vitreo-retinal interface and the anterior boundary of the second reflective layer, corresponding to the retinal pigment epithelium and the choriocapillaris. RNFL thickness was automatically assessed by computer assuming the correlation with the red highly reflective layer at the vitreo-retinal interface. The posterior margin of the RNFL was automatically located by starting within the photoreceptor layer (posterior) and searching forward in the image (19,26,27).

Throughout scanning, the patient kept both eyes constantly fixed on an internal target provided by the equipment. Each subject eye underwent fast RNFL and macula scan protocols. Mean OCT values were calculated from the values of the three scans. One of the authors (OA) performed the image acquisition and judged its quality. Scans with poor image quality were defined as scans with signal-to-noise

ratio of less than 45dB or excessive eye movement during measurement. We excluded three patients who had difficulty in cooperating with testing.

The fast RNFL scan protocol consisted of three consecutive 360° circular scans with a diameter of 3.4 mm centered on the optic disc, each containing 256 A-scans taken in a single session of 1.92 seconds. The parapapillary RNFL thickness parameters evaluated in this study were average thickness (360° measurement), temporal quadrant thickness (316° to 45°), superior quadrant thickness (46° to 135°), nasal quadrant thickness (136° to 225°), inferior quadrant thickness (226° to 315°), and thickness for each 12:00 position with the 3:00 as nasal, 6:00 position as inferior, 9:00 as temporal, and 12:00 position as superior.

The fast macula scan protocol consisted of six consecutive 6 mm radial line scans centered on the macula, each containing 128 A-scans taken in a single session of 1.92 seconds. Six sets of intersecting and equally spaced scans were obtained, each crossing the central fovea. The retinal thickness/volume tubular analysis program was used to evaluate macular scans. This analysis program presents mean foveal thickness and total macular volume in 3.5 and 6.00 mm macular maps. Macular retinal thickness data were displayed in three concentric circles. The central disk was the foveal region measuring 1.00 mm in diameter. The inner and outer rings were each divided into four quadrants; the rings had diameters of 3 mm and 6 mm, respectively, in 6.00 mm macular maps. An average retinal thickness and volume were reported for each of the nine regions.

Statistical Analysis

The data are reported as mean values ± standard deviation (SD). The differences between AD and control eyes were statistically evaluated with the Student *t* test. To assess whether a correlation existed between OCT, VEP, and clinical severity of disease, Pearson's correlation test was used. $P < 0.05$ was considered significant.

RESULTS

The mean ages of AD and control groups were 70.1 ± 9.7 years and 65.1 ± 9.8 years, respectively. There was no statistically significant difference in age and gender between groups. Demographic and clinical data of AD and control groups are shown in Table 1. Examples of OCT and VEP recordings from control and AD eyes are shown in Figure 1.

Optical Coherence Tomography

The mean RNFL average thickness was significantly reduced in AD patients (87.46 ± 23.78 microns) when compared with control subjects (113.16 ± 6.72 μm) ($P < 0.05$) (Table 2). The RNFL thickness in all quadrants and positions of AD patients was thinner than in control subjects. RNFL differences were statistically significant ($P < 0.05$) except in the temporal quadrant, 8:00 and 9:00 positions (Table 1).

The retinal thickness in all quadrants of the macula of AD patients was less than in control subjects. This thinning was prominent in the nasal, temporal, and inferior quadrants ($P < 0.05$) (Table 2). The macular volume of the AD patients was less than that of control subjects in all macular regions except the foveal minimum. The reduction in macular volume was statistically significant except in the nasal and inferior inner quadrants and the temporal and superior outer quadrants of the macula. The mean total macular volume of AD patients (6.80 ± 0.41 mm^3) was significantly reduced when compared with that of control subjects (7.10 ± 0.23 mm^3) ($P < 0.05$) (Table 1).

TABLE 1. *Demographic and clinical data of groups*

	AD	Control	*P* value
Age	70.1 ± 9.7	65.1 ± 9.8	0.180
(mean ± SD)	(52–83)	(49–79)	
Gender			0.837
Men	6	7	
Women	8	8	
MMSE	18.5 ± 6.3	29.4 ± 0.6	0.000*
(mean ± SD)	(8–28)	(29–30)	
VEP			
P100	107.96 ± 9.93	107.80 ± 10.40	0.950
Amplitude	16.35 ± 2.69	18 ± 3.59	0.053
	(12–23)	(14–24)	

*$P < 0.01$.

AD, Alzheimer disease; MMSE, Mini-Mental State Examination; SD, standard deviation; VEP, visual evoked potential.

Visual Evoked Potentials

No significant difference was found in the latencies and amplitudes of the VEP P100 of AD patients (107.96 ± 9.93 msec) (16.35 ± 2.69 μv) and control subjects (107.80 ± 10.40 msec) (18 ± 3.59 μv) ($P > 0.05$) (Table 1).

Correlation between Optical Coherence Tomography, Visual Evoked Potential, and Mini-Mental State Examination

A highly significant correlation was found between total macular volume and MMSE scores in AD patients (r = 0.696; $P = 0.006$) (Fig. 2). There was no correlation between OCT and VEP changes (Table 3).

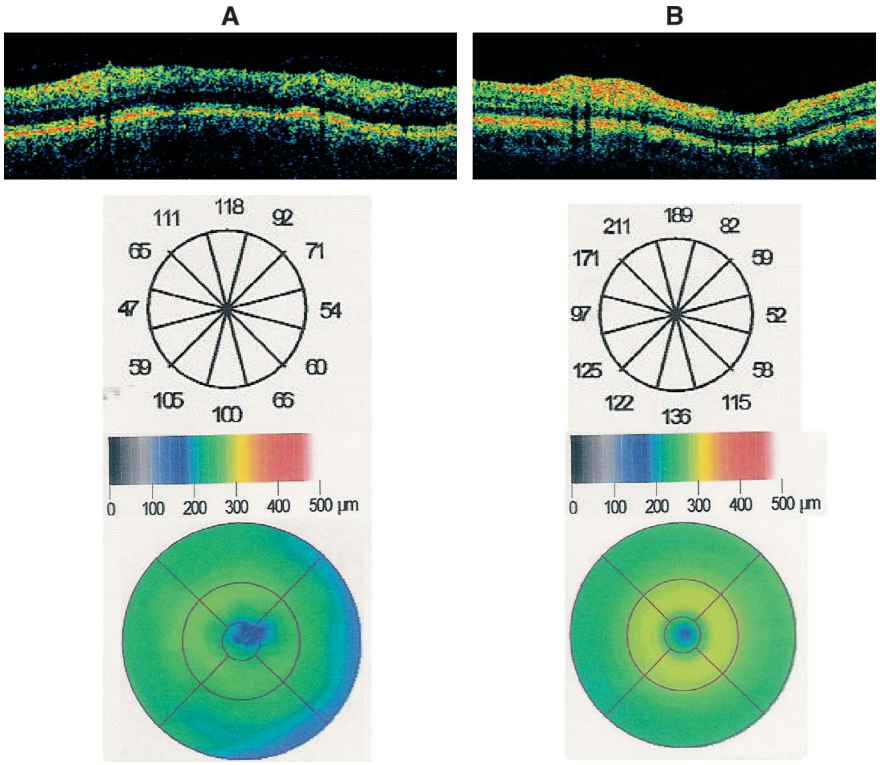

FIG. 1. Example of retinal nerve fiber layer (RNFL) thickness in one eye of a patient with Alzheimer disease (AD) **(A)** and one eye of a control subject **(B)**. Top: Circular optical coherence tomography (OCT) taken in cylindrical section of tissue surrounding the optic disc shows a marked decrease of the RNFL reflection in the eye of the AD patient **(A)** as compared with the eye of a control subject **(B)**. Bottom: The RNFL thickness in each clock position and the macular thickness in each region are reduced in the AD eye **(A)** as compared with the control subject eye **(B)**.

DISCUSSION

The results of our study suggest a significant reduction in parapapillary RNFL, macular thickness and volume in patients with AD. We have also demonstrated a highly significant correlation between total macular volume and MMSE scores. Structural changes were not significantly correlated to the VEP changes.

Our data are consistent with histologic studies (9,10) and other methods of evaluating the RNFL and optic nerve in vivo (15,28), which demonstrate substantial decline in the quantity of optic nerve fibers and a degeneration of retinal ganglion cells in AD. Optic disc pallor, pathologic disc cupping, and thinning of the neuroretinal rim and the RNFL have been reported in two clinical studies based on the subjective evaluation of fundus photographs (28,29). Tsai et al (28) have observed an increased cup-to-disc ratio, cup volume, and decreased disc rim area in AD patients by optic nerve analyzer. Parisi et al (15) demonstrated a reduction in RNFL thickness by using OCT and suggested that this morphologic abnormality is related to retinal dysfunction as revealed by abnormal PERG responses.

Our data indicate not only a significant decline in parapapillary RNFL but also in macular thickness and volume in AD eyes. These findings suggest a loss of retinal ganglion cells in AD patients. To our knowledge, no report has previously documented the macular volume and thickness in vivo in AD patients. These findings are in agreement with the postmortem study of Blanks et al (17) demonstrating a total decrease of 25% of neurons in the ganglion cell layer at the level of the foveal and parafoveal retina.

In the pathophysiology of AD, beta-amyloid peptides that are cleaved from the amyloid precursor protein (APP) play a critical role. In the later stages of the disease,

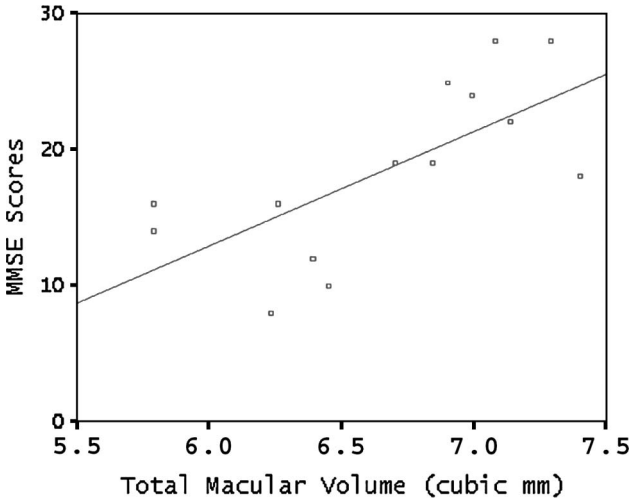

FIG. 2. Correlation plot of the total macular volume and Mini-Mental State Exam (MMSE) scores in our Alzheimer disease (AD) patients shows a high correlation (r = 0.696).

TABLE 2. ***Optical coherence tomography parameters of subjects***

Parameter	Location	Alzheimer group (n = 28), mean ± SD	Control group (n = 30), mean ± SD	*P*
Parapapillary RNFL thickness (microns)	RNFL (average)	87.46 ± 23.78	113.16 ± 6.72	**0.000**
	Superior RNFL	112.64 ± 35.32	137.16 ± 16.48	**0.002**
	Inferior RNFL	103.10 ± 33.64	141.56 ± 19.09	**0.000**
	Temporal RNFL	64.92 ± 17.70	72.30 ± 16.42	0.106
	Nasal RNFL	63.57 ± 19.09	96.00 ± 34.39	**0.000**
	1:00	103.53 ± 40.12	131.43 ± 24.22	**0.003**
	2:00	81.00 ± 27.87	114.13 ± 39.26	**0.001**
	3:00	49.96 ± 12.78	79.83 ± 39.20	**0.000**
	4:00	60.39 ± 22.59	95.33 ± 28.69	**0.000**
	5:00	87.17 ± 26.65	129.83 ± 31.85	**0.000**
	6:00	111.96 ± 38.01	153.83 ± 24.71	**0.000**
	7:00	111.17 ± 44.86	142.06 ± 26.35	**0.002**
	8:00	67.82 ± 21.69	74.03 ± 19.11	0.251
	9:00	51.03 ± 13.11	53.83 ± 12.33	0.406
	10:00	76.89 ± 23.95	90.16 ± 22.37	**0.033**
	Thickness at 11:00	117.14 ± 36.60	138.80 ± 27.23	**0.013**
	12:00	118.35 ± 40.53	142.03 ± 27.17	**0.013**
Average foveal/macular thickness (microns)	Foveal minimum	194.57 ± 30.54	165.26 ± 22.12	**0.000**
	Fovea	200.46 ± 20.74	218.25 ± 24.68	**0.004**
	Temporal inner macula	257.57 ± 21.14	267.96 ± 19.35	0.056
	Superior inner macula	269.60 ± 23.23	279.13 ± 12.05	0.060
	Nasal inner macula	265.46 ± 26.61	277.23 ± 14.51	**0.045**
	Inferior inner macula	264.78 ± 34.54	280.16 ± 11.78	**0.032**
	Temporal outer macula	224.57 ± 17.60	233.43 ± 14.17	**0.039**
	Superior outer macula	245.50 ± 13.01	247.70 ± 9.33	0.460
	Nasal outer macula	245.25 ± 21.82	264.93 ± 12.24	**0.000**
	Inferior outer macula	227.78 ± 23.07	241.36 ± 10.30	**0.007**
Foveal/macular volume (cubic mm)	Fovea	0.153 ± 0.01	0.160 ± 0.01	**0.005**
	Temporal inner macula	0.400 ± 0.03	0.420 ± 0.01	**0.006**
	Superior inner macula	0.418 ± 0.03	0.432 ± 0.01	0.081
	Nasal inner macula	0.413 ± 0.04	0.430 ± 0.02	0.068
	Inferior inner macula	0.410 ± 0.05	0.435 ± 0.01	**0.027**
	Temporal outer macula	1.197 ± 0.11	1.224 ± 0.06	0.272
	Superior outer macula	1.297 ± 0.06	1.315 ± 0.04	0.264
	Nasal outer macula	1.296 ± 0.11	1.394 ± 0.07	**0.000**
	Inferior outer macula	1.183 ± 0.10	1.267 ± 0.06	**0.000**
	Foveal minimum	6.809 ± 0.41	7.106 ± 0.23	**0.002**

RNFL, retinal nerve fiber layer; SD, standard deviation.

beta-amyloid peptides compose the characteristic pathologic findings of AD, including neurofibrillary tangles and neuritic plaques. The cortical degeneration characteristic of AD is present especially in visual association areas. Histopathologic studies have disclosed the pathologic hallmarks of AD (B-amyloid, tau, and APP neurofibrillary tangles and neuritic plaques) in subcortical visual centers, including the lateral geniculate nucleus and superior colliculus (31) but not in the retina (9,30). On the other hand, degeneration of retinal ganglion cells and their axons in the nerve fiber layer has been reported (10). Morphometric analysis has shown that in AD, the optic nerve has

TABLE 3. ***Correlations between visual evoked potential P100 latency, Mini-Mental State Examination score, and optic coherence tomography retinal thickness measures and optic coherence tomography parameters in Alzheimer disease***

Versus	RNFL average thickness	Foveal thickness	Total macular volume
VEP P100 latency			
Correlation coefficient (r)	0.318	−0.096	0.189
P	0.099	0.627	0.335
Mini-Mental State Examination score			
Correlation coefficient (r)	0.071	0.004	0.696
P	0.810	0.989	0.006

RNFL, retinal nerve fiber layer; VEP, visual evoked potential.

predominant loss of the largest class of retinal ganglion cells (M-cells) (10).

The loss of retinal ganglion cells may be a primary process or a consequence of retrograde neurodegeration occurring in the cortical regions.

We found no abnormalities in VEP in our AD patients. Normal pattern VEP responses have been described before in AD, although there is evidence that the P2 component of pattern VEP is delayed (32,33). In an earlier report, progressive increase in the latency of the flash VEP was related to the severity of dementia (33). These findings stem largely from the fact that flash VEP reflects the abnormality of visual association regions of the brain while pattern VEP shows the function of primary visual cortex and visual pathways (34). Sparing of the primary visual cortex with extensive cortical disease has been shown in AD (33) with positron emission tomography and histopathologic studies (35,36). The normal VEP responses in our study suggest that primary cortical region and optic nerve function is normal despite considerable RNFL loss.

The significant correlation we found between MMSE scores and macular volume as measured by OCT may be useful in providing a basis for further studies evaluating the effect of disease severity on RNFL.

REFERENCES

1. Hutton JT, Morris JL, Elias JW, Poston JN. Contrast sensitivity dysfunction in Alzheimer's disease. *Neurology* 1993;43:2328–30.
2. Gilmore GC, Wenk HE, Naylor LA, Koss E. Motion perception and Alzheimer's disease. *J Gerontol* 1994;49:P52–P57.
3. Trick GL, Silverman SE. Visual sensitivity to motion: age related changes and deficits in senile dementia of the Alzheimer's type. *Neurology* 1991;41:1437–40.
4. Cronin-Golomb A. Vision in Alzheimer's disease. *Gerontologist* 1995;35:370–76.
5. Cronin-Golomb A, Corkin S, Rizzo JF, Cohen J, Growdon JH, Banks KS. Visual dysfunction in Alzheimer's disease: relation to normal aging. *Ann Neurol* 1991;29:41–52.
6. Amstrong RA. Visual field defects in Alzheimer's disease patients may reflect differential pathology in the primary visual cortex. *Optom Vis Sci* 1996;73: 677–82.
7. Morrison JH, Hof PR, Bouras C. An anatomic substrate for visual disconnection in Alzheimer's disease. *Ann NY Acad Sci* 1991;640: 36–43.
8. Mountjoy CQ, Roth M, Evans NJ, Evans HM. Cortical neuronal counts in normal elderly controls and demented patients. *Neurobiol Aging* 1983;4:1–11.
9. Hinton DR, Sadun AA, Blanks JC, Miller CA. Optic nerve degeneration in Alzheimer's disease. *N Engl J Med* 1986; 315:485–7.
10. Sadun AA, Bassi CJ. Optic nerve damage in Alzheimer's disease. *Ophthalmology* 1990;97:9–17.
11. Curcio CA, Drucker DN. Retinal ganglion cells in Alzheimer's disease and aging. *Ann Neurol* 1993;33:248–57.
12. Davies DC, McCoubrie P, McDonald B, Jobst KA. Myelinated axon number in the optic nerve is unaffected by Alzheimer's disease. *Br J Ophthalmol* 1995;79:596–600.
13. Kergoat H, Kergoat MJ, Justino L, Chertkow H, Robillard A, Bergman H. An evaluation of the retinal nerve fiber layer thickness by scanning laser polarimetry in individuals with dementia of the Alzheimer type. *Acta Ophthalmol Scand* 2001;79:187–91.
14. Kergoat H, Kergoat MJ, Justino L, Robillard A, Bergman H, Chertkow H. Normal optic nerve head topography in the early stages of dementia of the Alzheimer type. *Dement Geriatr Cogn Disord* 2001;12:359–63.
15. Parisi V, Restuccia R, Fattapposta F, Mina C, Bucci MG, Pierelli F. Morphological and functional retinal impairment in Alzheimer's disease patients. *Clin Neurophysiol* 2001;112:1860–7.
16. Zeimer R, Asrani S, Zou S. Quantitative detection of glaucomatous damage at the posterior pole by retinal thickness mapping. A pilot study. *Ophthalmology* 1998;105:224–31.
17. Blanks JC, Torigoe Y, Hinton DR, Blanks RH. Retinal pathology in Alzheimer's disease. I. Ganglion cell loss in foveal/parafoveal retina. *Neurobiol Aging* 1996;17:377–84.
18. Guedes V, Schuman JS, Hertzmark E, Wollstein G, Correnti A, Mancini R, et al. Optical coherence tomography measurement of macular and nerve fiber layer thickness in normal and glaucomatous human eyes. *Ophthalmology* 2003;110:177–89.
19. Hee MR, Izatt JA, Swanson EA, Huang D, Schuman JS, Lin CP, et al. Optical coherence tomography of the human retina. *Arch Ophthalmol* 1995;113:325–32.
20. Hee MR, Puliafito CA, Wong C, Duker JS, Reichel E, Rutledge B, et al. Quantitative assessment of macular edema with optical coherence tomography. *Arch Ophthalmol* 1995;113:1019–2.
21. Hee MR, Puliafito CA, Wong C, Duker JS, Reichel E, Schuman JS, et al. Optical coherence tomography of macular holes. *Ophthalmology* 1995;102:748–56.
22. Krivoy D, Gentile R, Liebmann JM, Stegman Z, Rosen R, Walsh JB, et al. Imaging congenital optic disc pits and associated maculopathy using optical coherence tomography. *Arch Ophthalmol* 1996;114: 165–70.
23. McKhann G, Drachman D, Folstein M, Katzman R, Price D, Stadlan EM. Clinical diagnosis of Alzheimer's disease: report of the NINCDS-ADRDA Work Group under the auspices of the Department of Health and Human Services Task Force on Alzheimer's disease. *Neurology* 1984;34;939–44.
24. Morris JC. The Clinical Dementia Rating (CDR): current version and scoring rules. *Neurology* 1993;43:2412–13.

25. Folstein MF, Folstein SE, McHugh PR. "Mini-mental state". A practical method for grading the cognitive state of patients for the clinician. *J Psychiatr Res* 1975;12:189–98.
26. Huang D, Swanson EA, Lin CP, Schuman JS, Stinson WG, Chang W, et al. Optical coherence tomography. *Science* 1991;254: 1178–81.
27. Schuman JS. Optical coherence tomography for imaging and quantification of nerve fiber layer thickness. In: Schuman JS. *Imaging in Glaucoma*. Thorofare, NJ: Slack Inc; 1997:95–130.
28. Tsai CS, Ritch R, Schwartz B, Lee SS, et al. Optic nerve head and nerve fiber layer in Alzheimer's disease. *Arch Ophthalmol* 1991;109: 199–204.
29. Hedges TR, Perez Galves R, Speigelman D, Barbas NR, Peli E, Yardley CJ. Retinal nerve fiber layer abnormalities in Alzheimer's disease. *Acta Ophthalmol Scan* 1996;74:271–5.
30. Loffler KU, Edwards DP, Tso MO. Immunoreactivity against tau, amyloid precursor protein, and beta-amyloid in the human retina. *Invest Ophthalmol Vis Sci* 1995;36:24–31.
31. Leuba G, Saini K. Pathology of subcortical visual centres in relation to cortical degeneration in Alzheimer's disease. *Neuropathol Appl Neurobiol* 1995;21:410–22.
32. Harding GF, Wright CE, Orwin A. Primary presenile dementia: the use of the visual evoked potential as a diagnostic indicator. *Br J Psychiatry* 1985;147:532–9.
33. Orwin A, Wright CE, Harding GF, Rowan DC, Rolfe EB. Serial visual evoked potential recordings in Alzheimer's disease. *BMJ* 1986; 293:9–10.
34. Moore NC. Visual evoked responses in Alzheimer's disease: a review. *Clin Electroencephalogr* 1997;28:137–42.
35. Benson DF. The use of positron emission scanning techniques in the diagnosis of Alzheimer's disease. In: Corkin S, David KL, Growdon JH, Usdin E, Wurtman RJ, eds. *Alzheimer's Disease: A Report of Progress in Research*. New York: Raven Press; 1982:79–82.
36. Brun A, Gustafson L. Distribution of the cerebral degeneration in Alzheimer's disease. A clinico-pathological study. *Arch Psychiatr Nervenkr* 1976;223:15–33.